A Fuzzy Logic Control Strategy for Frequency and Voltage Regulation of the LLCL-Filter-Based Synchronverter System

Thai An Nguyen
Faculty of Electrical and Electronics Engineering, HCMC University of Technology and Education, Vietnam
ntan@hcmute.edu.vn (corresponding author)

Received: 22 July 2025 | Revised: 14 August 2025 and 5 September 2025 | Accepted: 6 September 2025

 DOI: https://doi.org/10.48084/etasr.13568

ABSTRACT

This paper proposes a control strategy employing Fuzzy Logic Control (FLC) to mitigate the voltage variation of the LLCL filter synchronverter system under various operating conditions, especially during an islanding scenario. The proposed strategy utilized an FLC-based adaptive control method for optimizing the integral coefficient of the reactive power control phase, the damping and virtual inertia coefficients, and defining a new approach in operating the reactive power control phase of the conventional LLCL filter synchronverter system. The proposed control strategy effectively suppresses the voltage variation phenomena during the off-grid operation, grid-connected modes, and islanding transitions while improving the frequency response under off-grid conditions and enhancing the output current performance under grid-tie scenarios. The simulations of the proposed control strategy of the LLCL filter synchronverter system are conducted in MATLAB/Simulink platform through various operating scenarios. The simulation results validated the improvements in voltage, frequency, and output current response compared to the conventional approach. Thus, enhancing the grid stability and power quality at the point of common coupling facilitates a more reliable integration of synchronverter-based distributed generation systems into modern power networks.

Keywords-synchronverter; adaptive control; virtual inertia; LLCL; FLC; VSG

I. INTRODUCTION

Transitioning to Renewable Energy Sources (RES) is one of the solutions to mitigate global warming and the reduction of fossil fuel reserves. The different nature characteristics of RES from traditional electrical power generations, which are mainly from synchronous generators, necessitate power electronic converter interfaces for grid integration. Despite being a solution in alternating fossil-fuel-based electrical generation, Converter-Interface Resources (CBR) still present distinct challenges when being integrated into electrical power systems [1-3].

Firstly, traditional power generation inherits the availability of primary sources to keep the generation stable, but due to the intermittent nature of primary sources, CBRs' generation is fully dependent on weather conditions and becomes uncertain [1, 4]. Therefore, the generation forecast must be carefully revised, and larger reserves need to be accounted for. Secondly, in most AC electrical power systems, inertia plays a vital role in keeping the system frequency stable under contingencies. In contrast, CBRs employing a Grid Following (GFL) control strategy for maximum harvesting of the primary sources result in lower system inertia [1-2, 5-7]. This reduction makes power systems more vulnerable to contingencies, especially under high integration of CBRs and low-load demand operating scenarios. Last but not least, ancillary services traditionally provided by synchronous generators are now becoming challenging for CBRs [1-3].

There have been studies with practical experiments aiming to mitigate the disadvantages of integrating CBRs into power systems. Soon after came the grid-supporting capability of CBRs, enabling certain functions to support the system under contingencies, as mentioned in [1-3, 5, 8]. Furthermore, advanced grid-supporting control strategies, e.g., virtual inertia, require an energy storage system to fulfill the supporting capability, such as a BESS [9–11], which will increase capital investment. Later, interest has been drawn to the Grid Forming (GFM) control strategy, which represents CBR models as voltage sources [1, 3, 6, 8, 12]. The GFM strategies are classified into four primary categories. Firstly, the droop control strategy [1, 3, 12], brings the capability of CBRs to adapt active and reactive power in response to system conditions. The Virtual Oscillator (VO) derives virtual inductance and capacitance elements to predict system frequency for control reference generation [13, 14].

Subsequently, studies focusing on the emulation of synchronous generator behavior led to the development of the Virtual Synchronous Generator (VSG) control strategy. The

VSG strategies are mainly categorized into two groups. The first group, called the Virtual Synchronous Machine, is based on the power swing equation to mimic the behavior of a synchronous generator. This control method was first introduced in [15] and further developed in [16-19]. The second is the synchronverter system, introduced in [20] and researched in [14, 21-25]. Authors in [22, 23] proposed a damping correction loop to mitigate transient phenomena and established mathematical frameworks for control parameter determination. In addition, authors in [14] introduced methodologies for coefficient determination aimed at mitigating oscillations in active and reactive power outputs. With regard to the adaptive control aspect, many works have been carried out, such as the switching sequence of controller values [24] and adaptive Fuzzy Logic Control (FLC) approaches [24, 25].

Authors in [25] developed an adaptive control strategy accompanied by FLC for the LLCL-filter synchronverter system to determine the damping coefficient (D_p) and virtual inertia (J_g) for better performance. However, voltage variations under off-grid and grid-tied conditions have not yet been addressed [25]. Moreover, deriving an adaptive FLC in the reactive power–voltage control phase that considers its interaction with the active power frequency control loop has not been investigated. Therefore, to overcome the limitations mentioned above, this paper proposes an adaptive control strategy for the LLCL-filter synchronverter system with the following contributions:

1. Deriving a central FLC to obtain adaptive values of the integral coefficient (K_g) in the reactive power control loop, together with the damping (D_p) and virtual inertia (J_g) in the active power loop.
2. Redefining of reactive power/voltage control modes under islanding operation of the synchronverter system.

II. THEORETICAL BACKGROUND AND THE PROPOSED ADAPTIVE FLC-BASED RPL CONTROL STRATEGY

A. Conventional Synchronverter Model

The synchronverter model was first introduced in [20] by emulating SG characteristics, using a (nonlinear) passive dynamic system. The synchronverter includes two main parts: the Active Power Loop (APL), which is responsible for controlling the active power output and angular frequency, and the Reactive Power Loop (RPL), which controls the terminal voltage and reactive power generation. The synchronverter system is defined by:

$$T_e = -M_f i_f \langle i, \frac{d\widetilde{cos\theta}}{dx} \rangle = M_f i_f \langle i, \widetilde{sin\theta} \rangle \quad (1)$$

$$e = \dot{\theta} M_f i_f \widetilde{sin\theta} \quad (2)$$

$$\begin{cases} P = \dot{\theta} M_f i_f \langle i, \widetilde{sin\theta} \rangle \\ Q = -\dot{\theta} M_f i_f \langle i, \widetilde{cos\theta} \rangle \end{cases} \quad (3)$$

where T_e, e, θ, P, and Q are the electromagnetic torque applied to the rotor, the three-phase generated voltage, the rotor angle, and the active and reactive power, respectively, i_f is the field excitation current, and M_f is the maximum mutual inductance between the virtual stator and the field winding. The synchronverter model [21-23] is defined by employing the damping correction loop in the APL:

$$J_g \frac{d\omega_g}{dt} = T_m - T_{ef} - D_p(\omega_g - \omega_g^*) - D_f \frac{d}{dt}\left(\frac{T_{ef}}{\psi_{ff}}\right) \quad (4)$$

$$K_g \frac{d\psi_f}{dt} = S_1(Q_t^* - Q_{tf}) + S_2\sqrt{\frac{2}{3}} D_q(U_t^* - U_{tf}) \quad (5)$$

where J_g is the inertia constant, T_m is the mechanical input torque, and ω_g* is the reference value of ω_g. The term D_p represents the frequency droop coefficient, D_q represents the voltage droop coefficient, K_g is the integral coefficient in the RPL, and D_f is the active damping factor.

In accordance with (4) and (5), the angular frequency follows the active power output of the synchronverter, mainly depending on the virtual inertia and damping coefficients. In addition, by controlling the virtual flux, the synchronverter can adjust the terminal voltage and reactive power generation transfer to the grid, which is achieved by varying the K_g coefficient in (5). Furthermore, the output active power/angular frequency and reactive power/voltage are related to each other via the virtual flux (ψ_f) of the synchronverter, emphasizing that the ability to control the virtual flux will affect the angular frequency.

B. LLCL Synchronverter System with FLC-Based Control Strategy

Authors in [25] proposed an LLCL-based synchronverter model that employs FLC [24-26] in the APL to adaptively determine both the virtual inertia and damping coefficient values, improving active power and angular frequency responses under various operating conditions. In addition, the model proposed in [25] replaced the common LCL filter with an LLCL filter due to its advantages in switching frequency cancellation and its smaller size [27]. Comparison and validation of the advantages of the proposed system over the conventional LCL-based synchronverter were also provided. Therefore, in this paper, the system presented in [25] is inherited, further developed, and compared through simulations with the newly proposed control strategy.

C. FLC-Based Adaptive Control Strategy for APL and RPL in LLCL Filter Synchronverter System

Authors in [25] proposed an adaptive control strategy by determining the values of D_p and J_g in the APL, but the integral coefficient (K_g) of the RPL was not considered. Active power output, angular frequency, reactive power, and terminal voltage of the synchronverter system are interrelated to some degree. Furthermore, the voltage and reactive power at the PCC were not mentioned or studied, especially in off-grid scenarios. If the terminal voltage and/or reactive power output are well regulated, they can help improve other parameters, such as output currents and/or angular frequency. Building upon the fuzzy inference system, along with insights from previous studies and a trial-and-error approach, an adaptive control strategy is proposed, where the FLC determines the adaptive

values of the three key coefficients, D_p, J_g, and K_g, within the RPL of the LLCL-filter synchronverter system. Furthermore, the proposed strategy redefines the control mode in the RPL through switches S1 and S2, in contrast to the configurations reported in [21-23]. The adaptive mechanism enables the real-time tuning of these coefficients to maintain optimal voltage stability and improve transient performance during dynamic changes in operating conditions. Specifically, during grid-tied operation, both switches S1 and S2 are set to ON to deliver the required reactive power and maintain the terminal voltage. Conversely, in islanded operation, switch S1 is set to OFF, allowing the strategy to prioritize terminal voltage control and ensure smooth voltage regulation during the transition.

The rule base for the applied FLC in order to obtain the K_g values in RPL along with the damping and virtual inertia coefficients in APL are based on the following general idea: In extreme scenarios, when frequency deviations are more than the deviations in terminal voltage, the inertia and damping should be set to high values and the integral coefficient should be at a medium value since the frequencies are of higher priority. On the other hand, when frequency deviations are less than the deviation of the terminal voltage, the integral coefficient of RPL (K_g) should be set to high values, lowering the damping and virtual inertia in the APL. Many trial-and-error runs were deployed for better output regulations. Tables I-III present the rule base of the adaptive FLC proposed in this study. Figure 1 shows the proposed adaptive FLC-based control strategy for the LLCL filter synchronverter system. Figure 2 demonstrates the membership functions of the inputs and outputs of the fuzzy inference system employed in the proposed strategy.

TABLE I. FUZZY RULE TABLE FOR DAMPING FACTOR

D_p		Frequency Deviation				
		NB	NS	ZE	PS	PB
Change of frequency deviation	NB	m	h	h	h	m
	NS	m	m	m	m	m
	ZE	l	l	l	l	l
	PS	m	m	m	m	m
	PB	m	h	h	h	m

TABLE II. FUZZY RULE TABLE FOR VIRTUAL INERTIA FACTOR

D_p		Frequency Deviation				
		NB	NS	ZE	PS	PB
Change of frequency deviation	NB	h	l	l	l	h
	NS	h	m	l	m	h
	ZE	m	l	l	l	m
	PS	h	m	l	m	h
	PB	h	m	l	m	h

TABLE III. FUZZY RULE TABLE FOR INTEGRAL FACTOR IN RPL

K_g		Voltage Deviation				
		NB	NL	Z	PL	PB
Frequency deviation	NB	H	H	H	M	h
	NS	M	H	M	L	h
	ZE	M	H	M	L	m
	PS	M	H	M	L	h
	PB	H	H	H	M	h

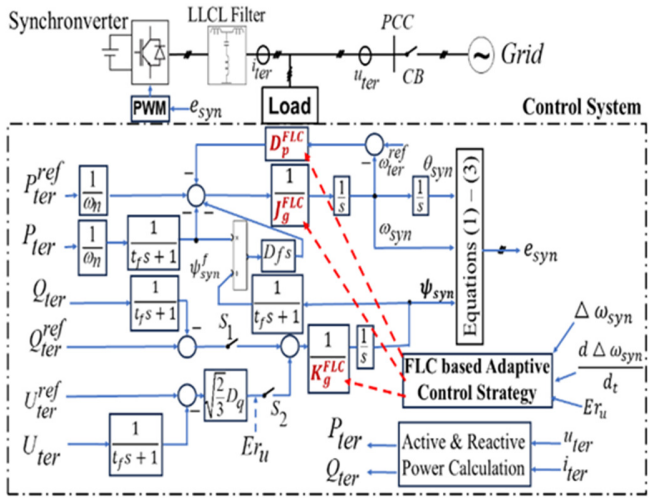

Fig. 1. The LLCL filter synchronverter system with proposed adaptive control strategy.

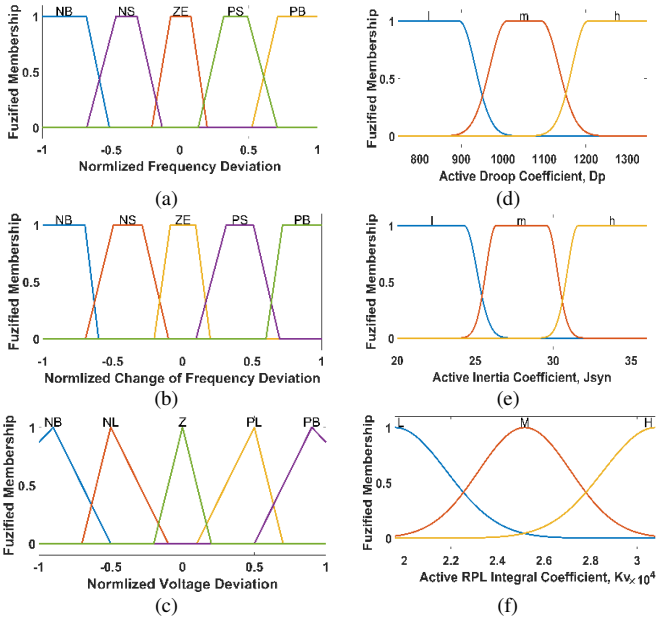

Fig. 2. Membership functions of inputs and outputs of the proposed FLC-based adaptive control strategy: (a) input membership functions of frequency deviation, (b) input membership functions of change of frequency deviation, (c) input membership functions of terminal voltage deviation, (d) output membership functions of adaptive damping coefficient, (e) output membership functions of adaptive inertia coefficient, (f) output membership functions of adaptive RPL integral coefficient.

III. SIMULATION SCENARIOS, RESULTS, AND DISCUSSION

A. Simulation Scenarios

The simulations comparing the proposed control strategy with the conventional LLCL filter synchronverter model in [25] were conducted under islanded and grid-tie operation modes in order to clarify the major advantages of the proposed strategy in improving terminal voltage variations and output current transients over the conventional mode. Furthermore, frequency variation improvement under grid-tie and islanded

scenarios is presented to evaluate the effectiveness of the proposed strategy. The entire simulation lasts for 5 s and includes two contingencies. At 1 s the synchronverter is disconnected from the power grid and works in islanded mode. Then at 3 s, the LLCL synchronverter system reconnects to the utility grid and operates in grid-tie mode. Table IV lists the system parameters under simulation in the MATLAB/Simulink platform.

TABLE IV. PARAMETERS OF THE LLCL SYNCHRONVERTER SYSTEM

Notation	Parameters	Values
Sb	Rated/base power	1.6 MVA
Vb	Rated/base line-line voltage	6.6 kV
fb	Rated/base frequency	60 Hz
ω_b	Rated/base angular frequency	377 rad/s
fsw	Switching frequency	12 kHz
Ts	Sampling time	833.33 ns
vDC	DC link voltage	13 kV
D_f	Active damping coefficient	1.13 Vs2/rad
D_q	RPL droop coefficient	3711 var/V
tf	Low-pass filter time constant	0.01 s

B. Results and Discussion

Simulations were carried out under the MATLAB/Simulink R2023b platform using an AMD RYZEN 5 core testing PC. The total real-time simulation of the proposed system and the conventional model are 2156 s and 1689 s, respectively. With the additional control targets in the proposed control strategy, an acceptable increase in simulation time by 27.6% occurred, which can be decreased with a more advanced PC.

Figure 3 shows the terminal voltage variations of the synchronverter system between the proposed strategy (blue line) and the conventional model (black line). The plots include the full simulation period, including islanding and reconnection to the utility. The conventional model shows voltage variations of nearly 15% under off-grid and islanding operation (Figure 3(a-c)), while the proposed strategy avoids this increase. Moreover, when reconnecting to the utility, the conventional model again exhibits noticeable changes in terminal voltage, as presented in Figure 3(d). In contrast, the proposed strategy keeps the voltage level almost unchanged throughout the simulation. Figures 4(a)-(b) exhibit the output and frequency variation during the off-grid scenario. Under islanded conditions, the current responses of both models are nearly identical. However, as indicated in (4, 5), variations in voltage and reactive power affect the angular frequency of the synchronverter system. With the proposed control strategy regulating the output voltage, the angular frequency response shows clear improvements in both settling time and oscillation magnitude. More specifically, the deviation from the rated value is reduced to 0.15% in the proposed model, compared to 0.25% in the original model. Furthermore, the frequency variation in the proposed model is more effectively damped, returning to the rated value more quickly, as illustrated in Figure 4(b). These results highlight the effectiveness of the proposed control scheme in enhancing system stability under islanding scenarios, ensuring faster dynamic recovery and reduced steady-state error compared to the conventional approach.

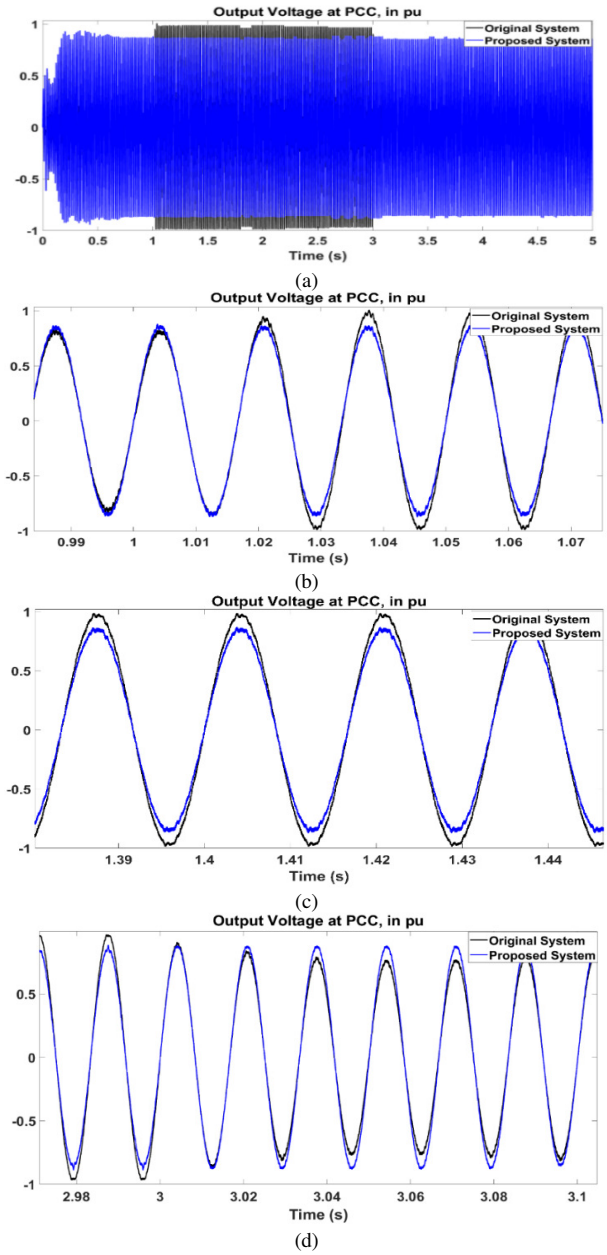

Fig. 3. Terminal voltage of the synchronverter system: (a) under the whole simulation period, (b) under the off-grid scenario, (c) during islanding operation, (d) under reconnecting operation.

Furthermore, a major improvement achieved by the proposed strategy is the significant reduction of the transient current value when reconnecting the synchronverter system to the utility. In detail, the conventional model endured a very high output current of up to 4.2 pu in the first cycle, and then decreased to 2 pu within 4 cycles, as depicted in Figure 5(a). In contrast, with the proposed control strategy that regulates K_g, D_p, and J_g coefficients in the APL and RPL, terminal voltages are stably regulated. Then the output currents in the proposed control model are improved by rising to 1.6 pu and gradually lowering to 1 pu within 5 cycles (less than 0.1 s). On the other hand, the frequency variation in this period of the two models

is quite the same, and deviations are much smaller than 0.2% of the rated frequency, as presented in Figure 5(b).

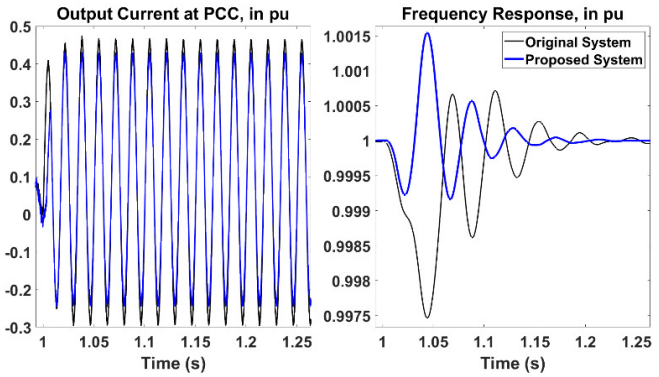

Fig. 4. Responses of (a) output current and (b) frequency of the synchronverter system under the off-grid scenario.

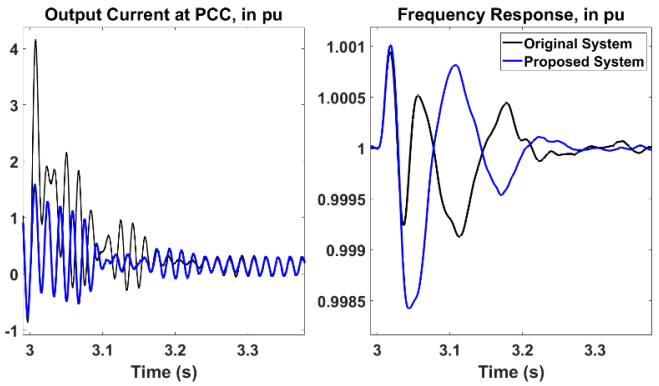

Fig. 5. Responses of (a) output current and (b) frequency of the synchronverter system under reconnecting to the utility.

IV. CONCLUSION

In this paper, an adaptive control strategy based on FLC for an LLCL filter synchronverter system has been proposed and investigated. The aim is to implement an FLC-based approach capable of adaptively determining the integral coefficient in the RPL, as well as the damping and virtual inertia coefficients in the APL, along with a modification of the RPL control mode. The proposed control system adaptively includes all three coefficients in a single FLC-based controller, which has not been investigated or applied in any previous research. Based on the simulation results, the outcomes of the proposed control strategy have been validated by overcoming the voltage variation problems observed in the conventional control model under different operating conditions. Furthermore, the proposed strategy yields significant improvements in both frequency response and transient output currents of the Synchronverter system, compared with the conventional LLCL filter Synchronverter model.

ACKNOWLEDGMENT

This research was supported by the Ho Chi Minh City University of Technology and Education, Vietnam.

REFERENCES

[1] M. Tozak, S. Taskin, I. Sengor, and B. P. Hayes, "Modeling and Control of Grid Forming Converters: A Systematic Review," *IEEE Access*, vol. 12, pp. 107818–107843, Aug. 2024, https://doi.org/10.1109/ACCESS.2024.3437236.

[2] Denholm, T. Mai, R. W. Kenyon, B. Kroposki, and M. O'Malley, *Inertia and the Power Grid: A Guide Without the Spin*, 1st ed. Golden, CO, USA: National Renewable Energy Laboratory, 2020.

[3] S. Yari, I. Kamwa, and D. Rimorov, "Comparison of Grid-Following and Grid-Forming Inverters Performance for Frequency Stability in Power Systems: A Dynamic Study," in *2024 IEEE Canadian Conference on Electrical and Computer Engineering (CCECE)*, Dec. 2024, pp. 363–368, https://doi.org/10.1109/CCECE59415.2024.10667285.

[4] G. Tran, T. A. Nguyen, M. V. N. Hoang, N. A. Nguyen, and T. T. Tran, "Load Shedding in High-Integrated Wind Energy Power Systems Using Voltage Electrical Distance," *Engineering, Technology & Applied Science Research*, vol. 12, no. 2, pp. 8402–8409, Apr. 2022, https://doi.org/10.48084/etasr.4779.

[5] H. Ruan, Y. Xiao, H. Luo, Y. Yang, M. Molinas, and H. Luo, "Optimized Parameter Design of Grid-Following and Grid-Forming Converters for Wide Operating Region," *IEEE Journal of Emerging and Selected Topics in Power Electronics*, vol. 13, no. 4, pp. 5218–5233, Dec. 2025, https://doi.org/10.1109/JESTPE.2025.3535769.

[6] R. H. Lasseter, Z. Chen, and D. Pattabiraman, "Grid-Forming Inverters: A Critical Asset for the Power Grid," *IEEE Journal of Emerging and Selected Topics in Power Electronics*, vol. 8, no. 2, pp. 925–935, Jun. 2020, https://doi.org/10.1109/JESTPE.2019.2959271.

[7] T. A. Trivedi, R. Jadeja, and P. Bhatt, "A Review on Direct Power Control for Applications to Grid Connected PWM Converters," *Engineering, Technology & Applied Science Research*, vol. 5, no. 4, pp. 841–849, Aug. 2015, https://doi.org/10.48084/etasr.544.

[8] Z. Zou *et al.*, "Modeling and Control of a Two-Bus System With Grid-Forming and Grid-Following Converters," *IEEE Journal of Emerging and Selected Topics in Power Electronics*, vol. 10, no. 6, pp. 7133–7149, Sep. 2022, https://doi.org/10.1109/JESTPE.2022.3182366.

[9] P. Imgart, A. Narula, M. Bongiorno, M. Beza, and J. R. Svensson, "External Inertia Emulation to Facilitate Active-Power Limitation in Grid-Forming Converters," *IEEE Transactions on Industry Applications*, vol. 60, no. 6, pp. 9145–9156, Aug. 2024, https://doi.org/10.1109/TIA.2024.3443792.

[10] M. Almas Prakasa, I. Robandi, R. Nishimura, and M. Ruswandi Djalal, "A Hybrid Controlling Parameters of Power System Stabilizer and Virtual Inertia Using Harris Hawk Optimizer in Interconnected Renewable Power Systems," *IEEE Access*, vol. 12, pp. 76219–76243, May. 2024, https://doi.org/10.1109/ACCESS.2024.3405994.

[11] M. Chethan and K. Ravi, "Virtual Inertia Support for Renewable Energy Integration: A Review," *IEEE Access*, vol. 13, pp. 11517–11531, Jun. 2024, https://doi.org/10.1109/ACCESS.2024.3416694.

[12] Y. Lin *et al.*, *Research Roadmap on Grid-Forming Inverters*, 1st ed. Golden, CO, USA: National Renewable Energy Laboratory, Nov. 2020.

[13] M. A. Awal and I. Husain, "Unified Virtual Oscillator Control for Grid-Forming and Grid-Following Converters," *IEEE Journal of Emerging and Selected Topics in Power Electronics*, vol. 9, no. 4, pp. 4573–4586, Dec. 2021, https://doi.org/10.1109/JESTPE.2020.3025748.

[14] H. Yin, S. Wang, and Z. Zhou, "Synchronverters With a Virtual Oscillator to Attenuate Power Oscillations," *IEEE Journal of Emerging and Selected Topics in Power Electronics*, vol. 12, no. 2, pp. 1303–1310, Apr. 2024, https://doi.org/10.1109/JESTPE.2023.3329010.

[15] Y. Chen, R. Hesse, D. Turschner, and H.-P. Beck, "Improving the grid power quality using virtual synchronous machines," in *2011 International Conference on Power Engineering, Energy and Electrical Drives*, Feb. 2011, pp. 1–6, https://doi.org/10.1109/PowerEng.2011.6036498.

[16] G. W. Chang and K. T. Nguyen, "A New Adaptive Inertia-Based Virtual Synchronous Generator with Even Inverter Output Power Sharing in Islanded Microgrid," *IEEE Transactions on Industrial Electronics*, vol.

71, no. 9, pp. 10693–10703, Sep. 2024, https://doi.org/10.1109/TIE.2023.3327515.

[17] G. Ala *et al.*, "Virtual Synchronous Generator: An application to Microgrid Stability," in *2022 11th International Conference on Renewable Energy Research and Application (ICRERA)*, Sep. 2022, pp. 151–157, https://doi.org/10.1109/ICRERA55966.2022.9922782.

[18] G. Ala *et al.*, "Governing Microgrid Stability: An Application of Virtual Synchronous Generator," in *2024 12th International Conference on Smart Grid (icSmartGrid)*, Feb. 2024, pp. 504–511, https://doi.org/10.1109/icSmartGrid61824.2024.10578285.

[19] M. Ebrahimi, S. A. Khajehoddin, and M. Karimi-Ghartemani, "An Improved Damping Method for Virtual Synchronous Machines," *IEEE Transactions on Sustainable Energy*, vol. 10, no. 3, pp. 1491–1500, Jul. 2019, https://doi.org/10.1109/TSTE.2019.2902033.

[20] Q.-C. Zhong and G. Weiss, "Synchronverters: Inverters That Mimic Synchronous Generators," *IEEE Transactions on Industrial Electronics*, vol. 58, no. 4, pp. 1259–1267, Apr. 2011, https://doi.org/10.1109/TIE.2010.2048839.

[21] Q.-C. Zhong, P.-L. Nguyen, Z. Ma, and W. Sheng, "Self-Synchronized Synchronverters: Inverters Without a Dedicated Synchronization Unit," *IEEE Transactions on Power Electronics*, vol. 29, no. 2, pp. 617–630, Oct. 2014, https://doi.org/10.1109/TPEL.2013.2258684.

[22] S. Dong and Y. C. Chen, "Adjusting Synchronverter Dynamic Response Speed via Damping Correction Loop," *IEEE Transactions on Energy Conversion*, vol. 32, no. 2, pp. 608–619, Jun. 2017, https://doi.org/10.1109/TEC.2016.2645450.

[23] S. Dong and Y. C. Chen, "A Method to Directly Compute Synchronverter Parameters for Desired Dynamic Response," *IEEE Transactions on Energy Conversion*, vol. 33, no. 2, pp. 814–825, Jun. 2018, https://doi.org/10.1109/TEC.2017.2771401.

[24] K. Y. Yap, C. M. Beh, and C. R. Sarimuthu, "Fuzzy logic controller-based synchronverter in grid-connected solar power system with adaptive damping factor," *Chinese Journal of Electrical Engineering*, vol. 7, no. 2, pp. 37–49, Jun. 2021, https://doi.org/10.23919/CJEE.2021.000014T.

[25] Tran, D. Phan Quoc, B. Nguyen, and Y. Weng Kean, "The LLCL filter-based synchronverter with adaptive fuzzy logic controller," *International Journal of Power Electronics and Drive Systems (IJPEDS)*, vol. 15, Dec. 2024, Art. no. 2115, https://doi.org/10.11591/ijpeds.v15.i4.pp2115-2127.

[26] V. T. Ha, "Torque Control of an In-Wheel Axial Flux Permanent Magnet Synchronous Motor using a Fuzzy Logic Controller for Electric Vehicles," *Engineering, Technology & Applied Science Research*, vol. 13, no. 2, pp. 10357–10362, Apr. 2023, https://doi.org/10.48084/etasr.5689.

[27] W. Wu, Y. He, and F. Blaabjerg, "An LLCL Power Filter for Single-Phase Grid-Tied Inverter," *IEEE Transactions on Power Electronics*, vol. 27, no. 2, pp. 782–789, Oct. 2012, https://doi.org/10.1109/TPEL.2011.2161337.